ELSEVIER

In vitro evaluation of electrospun silk fibroin scaffolds for vascular cell growth

Xiaohui Zhang [a], Cassandra B. Baughman [b], David L. Kaplan [a,b,*]

[a] *Departments of Chemical and Biological Engineering and Biomedical Engineering, Tufts University, 4 Colby Street, Medford, MA 02155, USA*
[b] *Tufts University School of Medicine, Sackler School of Graduate Biomedical Science, Department of Anatomy and Cell Biology, Boston, MA 02111, USA*

Abstract

Human aortic endothelial (HAEC) and human coronary artery smooth muscle cell (HCASMC) responses on electrospun silk fibroin scaffolds were studied to evaluate potential for vascular tissue engineering. Cell proliferation studies supported the utility of this biomaterial matrix by both HAECs and HCASMCs. Alignment and elongation of HCASMCs on random non-woven nanofibrous silk scaffolds was observed within 5 days after seeding based on SEM and confocal microscopy. Short cord-like structures formed from HAECs on the scaffolds by day 4, and a complex interconnecting network of capillary tubes with identifiable lumens was demonstrated by day 7. The preservation of cell phenotype on the silk fibroin scaffolds was confirmed by the presence of cell-specific markers, including CD146, VE-cadherin, PECAM-1 and vWF for HAECs, and SM-MHC2 and SM-actin for HCASMCs at both protein and transcription levels using immunocytochemistry and real-time RT-PCR, respectively. Formation of ECM was also demonstrated for the HCASMCs, based on the quantification of collagen type I expression at protein and transcription levels. The results indicate a favorable interaction between vascular cells and electrospun silk fibroin scaffolds. When these results are factored into the useful mechanical properties and slow degradability of this protein biomaterial matrix, potential utility in tissue-engineered blood vessels can be envisioned.
© 2008 Elsevier Ltd. All rights reserved.

Keywords: Silk; Electrospinning; Endothelial cells; Smooth muscle cells; Vascular

1. Introduction

Acute thrombogenicity, anastomotic intimal hyperplasia, aneurysm formation, infection, and progression of atherosclerotic disease result in low patency of small-diameter (<6 mm) prosthetic vascular grafts after surgical operations [1]. To address these needs, different design criteria are required than for larger diameter systems. Tissue engineering offers an alternative approach to address the need for small-diameter vascular grafts through the design of non-thrombogenic interfaces, such as endothelial monolayers [2]. However, only a few systems have achieved promising clinical results.

A blood vessel substitute with the required functional characteristics of a normal blood vessel, including non-thrombogenic, vasoactivity and appropriate mechanical properties to match native vessels, remains to be demonstrated [3].

Biodegradable synthetic polymer scaffolds from polyglycolic acid (PGA) [4], poly-L-lactic acid [4], polyhydroxyalkanoates [5] such as poly-4-hydroxybutyrate [6], polycaprolactone-*co*-polylactic acid [7], and polyethylene glycol [8] have been explored with this goal in mind. However, premature loss of mechanical strength because of the failure of cells to produce requisite ECM before polymer degradation would be a potential risk. Success with a hybrid scaffold consisting of a PGA sheet and a polycaprolactone-*co*-polylactic acid copolymer was achieved clinically, but only in relatively low-pressure pulmonary circulation ($\approx 20-30$ mm Hg during systole) [7], a less demanding flow environment than the higher-pressure coronary artery ($\approx 100-140$ mm Hg during systole) [9]. Natural

* Corresponding author. Departments of Chemical and Biological Engineering and Biomedical Engineering, Tufts University, 4 Colby Street, Medford, MA 02155, USA. Tel.: +1 617 627 3251; fax: +1 617 627 3231.
E-mail address: david.kaplan@tufts.edu (D.L. Kaplan).

polymers such as collagen and fibrin have also been utilized to construct biological vascular grafts, populated and compacted by smooth muscle cells, and exhibiting high tensile strength and flexibility [10]. However, even with reinforcement by a Dacron mesh, the burst strength of these constructs was lower than the burst strength of human saphenous veins (1680 ± 307 mm Hg), the gold standard for bypass grafts.

To address challenging mechanical environments, while fostering slow degradation and remodeling into native tissue, we have been exploring silk fibroin-based biomaterials for a number of tissue needs [11,12]. Silks offer unique mechanical properties in different material formats, excellent biocompatibility, controlled degradability, and versatile processability, thus offering potential for tissue engineering applications. Moreover, the ability to process silk into different structural formats using an all-aqueous process render it useful for the delivery of bioactive components via this biomaterial matrix, as well as avoiding concerns for residual organic solvents in the devices. Along these lines, we recently fabricated small-diameter silk fibroin tubular scaffolds by electrospinning [13]. These scaffolds demonstrated structural integrity and the ability to withstand arterial pressures in a similar mode to native vessels.

In the present study, electrospun silk fibroin scaffolds (ESFS) were studied for vascular cell responses *in vitro*. Electrospinning produces a network of nanofibers to partly mimic the structure of the ECM. The aim of the present study was to characterize the potential of these nanofiber silk matrices to support vascular smooth muscle cell and endothelial cell functions. A good vascular scaffold for grafting would promote cell−scaffold interactions and maintain cell phenotype during the culture period. Human coronary artery smooth muscle cells (HCASMCs) and human aortic endothelial cells (HAECs) were studied for changes in cell morphology, viability, proliferation and phenotype. The ECM production of smooth muscle cells was also examined at both genetic and protein expression levels. The results support the utility of these silk fibroin nanofiber matrices as potential scaffolds for vascular tissue engineering needs.

2. Experimental

2.1. Materials

Cocoons of *Bombyx mori* silkworm were kindly supplied by Tajima Shoji Co. (Yokohama, Japan). Poly (ethylene oxide) (PEO) with an average molecular weight of 900,000, Triton X-100 and 10% neutral buffered formalin solution were purchased from Sigma−Aldrich (St. Louis, MO). Fetal bovine serum (FBS), Dulbecco's phosphate buffered saline (D-PBS) without calcium or magnesium and trypsin were from Gibco (Carlsbad, CA). Smooth muscle cell medium (SMCM) with growth supplement was from ScienCell Research Laboratories (Carlsbad, CA). Endothelial growth medium-2 (EGM-2) was from Lonza (Walkersville, ML). All other substances were of analytical or pharmaceutical grade and obtained from Sigma−Aldrich.

2.2. Preparation of regenerated B. mori silk fibroin solutions

B. mori silk fibroin solutions were prepared as previously described [14]. Briefly, cocoons of *B. mori* were boiled for 30 min in an aqueous solution of 0.02 M Na_2CO_3, and then rinsed thoroughly with distilled water to extract the glue-like sericin proteins. The extracted silk fibroin was then dissolved in 9.3 M LiBr solution at 60 °C for 4 h, yielding a 20% (w/v) solution. This solution was dialyzed against distilled water using a Slide-a-Lyzer dialysis cassette (MWCO 3500, Pierce) at room temperature for 48 h to remove the salts. The dialysate was centrifuged for 20 min at 5 °C twice to remove impurities and aggregates that formed during dialysis. The final concentration of silk fibroin aqueous solution was approximately 8% (w/v). This concentration was determined by weighing the residual solid of a known volume of solution after drying at 60 °C for 24 h.

2.3. Preparation of spinning solution

Silk/PEO blends in water were prepared by adding 5.0% (w/v) PEO (900,000 g/mol) into 8.0% (w/v) silk fibroin aqueous solution with a volume ratio of 1:4, which generated 7.5% (w/v) silk/PEO solutions. Homogeneous PEO solutions of 5% (w/v) were obtained by adding PEO to distilled water and stirring for 2 days at room temperature. The silk/PEO mixing solutions were stirred gently to avoid the premature formation of β-sheet structure during blending.

2.4. Electrospinning

Electrospinning was performed with a steel capillary tube with a 1.5 mm inside diameter tip mounted on an adjustable, electrically insulated stand as described earlier [15]. The capillary tube was maintained at a high electric potential for electrospinning and mounted in the parallel plate geometry. The capillary tube was connected to a syringe filled with a silk/PEO blend solution. A constant volume flow rate was maintained using a syringe pump. The electric potential, solution flow rate and the distance between the capillary tip and the collection plate were adjusted so that a stable jet was obtained without dripping. The electrospun fibers were collected on a collection plate covered with aluminum foil. The electrospun non-woven mats were treated with 100% methanol for 10 min to induce a β-sheet conformational transition, which results in insolubility in water. The PEO was removed from the mats by leaching in distilled water at room temperature for 72 h.

2.5. In vitro culture of vascular cells on ESFS

The HAECs (Clonetics, Walkersville, ML) at passage 5 and immortalized HCASMCs at passage 13 (24 years old donor, female, no vascular disease), (Tufts-New England Medical Center, Boston, MA) were used to evaluate the capability of electrospun silk fibroin scaffold for supporting vascular cells and maintaining phenotype. The HAECs and HCASMCs were cultured in endothelial growth medium-2 (EGM-2, Lonza, Walkersville, ML) supplemented with 10% fetal bovine serum (FBS), and smooth muscle cell medium (SMCM, ScienCell Research Laboratories, Carlsbad, CA) with 10% FBS, 1% smooth muscle cell growth supplement (SMCGS) and 1% penicillin/streptomycin solution (P/S), respectively. The medium was replaced every 2 days and the cultures were maintained in a humidified incubator at 37 °C and 5% CO_2.

Electrospun silk fibroin scaffolds were punched into small discs with a diameter of 1.43 cm (9/16 inch) to fit 24-well cell culture plates and sterilized by immersion in 70% ethanol for 30 min. The scaffolds were washed 3 times with sterile PBS and transferred to 24-well non-treated cell culture plates (BD Biosciences, San Jose, CA) to increase cell−matrix interactions and to reduce cell attachment on the plates. The scaffolds were incubated in 1 ml of cell culture medium at 37 °C overnight before cell seeding to saturate the scaffold with growth medium and improve cell attachment. The cells were seeded at the density of 7.5×10^4 cells/cm^2 for HAECs and 2.5×10^5 cells/cm^2 for HCASMCs in EGM-2 and SMCM on the pre-wetted electrospun scaffolds, respectively. One milliliter of culture medium was used for each well and the medium was changed every 2 days over 14 days for the HAECs and 36 days for the HCASMCs, respectively.

2.6. Scanning electron microscopy (SEM)

SEM was used to study cell morphology on the ESFS. Following harvest, the seeded silk scaffolds were washed with PBS 3 times and fixed in 10%

neutral buffered formalin solution (Sigma–Aldrich, St. Louis, MO) at 4 °C. Fixed samples were dehydrated through exposure to a gradient of alcohol (25, 50, 75, 85, 95 and 100%) followed by air drying in a fume hood. Specimens were examined using a LEO Gemini 982 Field Emission Gun SEM (Thornwood, NY).

2.7. DNA content assay

To study cell proliferation on the nanofibrous scaffolds, viable cells were determined by Pico green™ DNA content assay (Molecular Probes, Carlsbad, CA). Briefly, the scaffolds ($n = 3$) were rinsed 3 times with PBS and collected in 1.5 ml Eppendorf tubes and stored at −80 °C. Frozen scaffolds were cut into small pieces and lysed in 200 μL 0.2% (v/v) Triton X-100 and 5 mM MgCl$_2$ for 30 min to release the DNA into the solution. After centrifugation at 12,000 rpm for 10 min, 4 °C, the supernatants were collected for assay. DNA content was determined fluorometrically at excitation wavelength of 480 nm and emission wavelength 528 nm using a Fluoroskan Ascent FL spectrofluorometer (Thermo Life Sciences, Basingstoke, UK). The amount of DNA was calculated by interpolation from a standard curve prepared using lambda DNA in 10 mM Tris–HCl (pH 7.4), 5 mM NaCl, 0.1 mM EDTA over a range of concentrations.

2.8. Cell viability and metabolism activity assay

The viability of the HAECs and HCASMCs on the scaffolds was examined by live/dead assay (Molecular Probes, Eugene, OR). Briefly, scaffolds seeded with cells were washed with PBS, incubated in 2 mM calcein AM (staining live cells) and 4 mM EthD-1 (staining dead cells) in PBS for 30 min at room temperature. The cells were then washed again with PBS before imaging using a Leica DMIRE2 confocal microscope with a TCS SP2 scanner (Leica Microsystems, Manheim/Wetzlar, Germany) at excitation of 495 nm and emission of 515 nm. The metabolic activity of the cultured cells on scaffolds was assessed by monitoring alamarBlue™ (Invitrogen Corporation, Carlsbad, CA) reduction at the end of the incubation period. Briefly, the scaffolds were washed with PBS and transferred to a 12-well cell culture plate. A volume of 1 ml fresh medium and 100 μL alamarBlue™ were added to each well and incubated for 2 h at 37 °C and 5% CO$_2$. Triplicate 100-μL aliquots of culture medium were taken from each culture scaffold and transferred to a 96-well assay plate. Fluorescence was measured using a fluorometer with excitation and emission filters at 540 and 590 nm, respectively.

2.9. Immunocytochemisty analyses

Immediately after harvest, the scaffolds were washed in PBS and fixed in 10% neutral buffered formalin before immunohistochemical analysis. The fixed samples were rinsed 3 times in PBS and incubated with 0.1% (v/v) Triton X-100 in PBS for 15 min at room temperature. The samples were then washed 3 times in PBS and incubated with horse serum (Vector Laboratories, Burlingame, CA) for 20 min at room temperature to block non-specific binding. Afterwards, scaffolds seeded with HAECs and HCASMCs were incubated with different primary antibodies (Table 1) at 4 °C overnight in a humidified chamber, respectively. After washing 3 times with PBS, the samples were reacted with secondary antibody Alexa Fluor® 488 goat anti-mouse IgG (H + L)

Table 1
Antibodies for immunocytochemistry assay

Cell type	Antibody	Dilution	Company
HCASMCs	SM-MHC2	1:250	Abcam, Cambridge, MA
	SM-actin	1:100	Chemicon, Temecula, CA
	COL I	1:100	Chemicon, Temecula, CA
	Elastin	1:100	Chemicon, Temecula, CA
HAECs	CD146	1:500	Chemicon, Temecula, CA
	VE-C	1:10	Chemicon, Temecula, CA
	PECAM-1	1:50	Chemicon, Temecula, CA

(1:250 dilution, Invitrogen Corporation, Carlsbad, CA) for 1 h at room temperature. Then the samples were washed 3 times with PBS and observed under a confocal laser scanning microscope (TCS SP2, Leica Microsystems, Germany). Controls included leaving out the primary antibody to confirm non-specific binding.

2.10. Real-time RT-PCR analysis

Total RNA was extracted from cells using an RNeasy Mini Kit (Qiagen, Valencia, CA, USA) following the supplier's instructions. Briefly, electrospun scaffolds ($n = 3$) were harvested and washed in PBS, transferred into 2-ml Eppendorf tubes and kept in RNA later solution at −20 °C. After thawing, the tubes were centrifuged at 12,000g for 10 min to pellet the cells and scaffolds. The supernatants were removed and the scaffolds were cut into small pieces before being lysed in 350 μL buffer RLT (Qiagen, Valencia, CA) with 1% β-mercaptoethanol (β-ME). The supernatants of the lysates after centrifugation were collected and homogenized with a QIAshredder spin column (Qiagen, Valencia, CA) and then 350 μL of 70% ethanol (v/v) was added to the supernatant and applied to an RNeasy mini spin column (Qiagen, Valencia, CA) to wash and elute RNA. The total concentration of RNA extracted was determined using Ultraviolet spectroscopy (UV) at OD = 260 nm and reverse transcription reactions were performed with 50 ng total RNA using high-capacity cDNA archive kit (Applied Biosystems, Foster City, CA) following the supplier's instructions.

Customized probe-based Taqman gene expression (Applied Biosystems, Foster City, CA) was used for the real-time RT-PCR reactions and the reactions were conducted with an ABI 7000 Sequence Detection System (Applied Biosystems, Foster City, CA) at 50 °C for 2 min, 95 °C for 10 min, followed by 50 cycles of amplifications, consisting of a denaturation step at 95 °C for 15 s, and extension step at 60 °C for 1 min. The expression level of the target genes was normalized to the housekeeping gene, glyceraldehyde-3-phosphate dehydrogenase (GAPDH) using the 2ΔCt formula. The genes of CD146, vWF, VE-cadherin for HAECs and collagen type I and elastin for HCASMCs were selected and each sample was analyzed in triplicate.

2.11. Statistical analysis

Values (at least triplicate) were averaged and expressed as mean ± standard deviation (SD). Statistical differences were determined by Student's two-tailed t test. Differences were considered statistically significant at $p < 0.05$.

3. Results and discussions

3.1. Morphology of silk electrospun nanofibrous scaffold

The silk electrospun nanofibrous scaffolds were prepared as previously reported [16] to generate solid nanofibers free of beading. PEO was used to aid the electrospinning process by increasing the viscosity and surface tension of the electrospinning solution, which was also used for electrospinning of other proteins such as collagen [16], elastin [17] and gelatin [18]. Methanol treatment was employed after spinning to induce β-sheet structure to provide insolubility of the silk scaffolds in aqueous solution. The morphology and diameters of the electrospun fibers before and after PEO extraction were examined by SEM (Fig. 1). The fibrous scaffolds consisted of randomly oriented fibers with diameters ranging from 170 to 890 nm. The distribution of the fiber diameters was determined with an average of about 377 ± 70 nm (Fig. 2). The SEM micrographs showed that the nanofibers had a solid surface with interconnected voids among the fibers, presenting
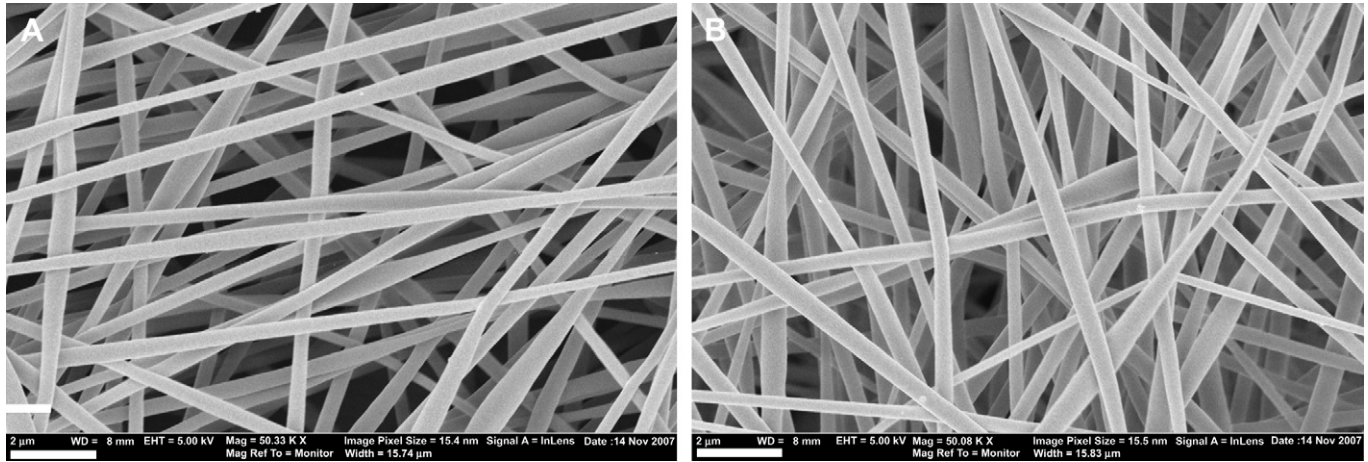
Fig. 1. SEM micrographs of electrospun silk fibroin scaffolds: (A) PEO non-extracted scaffold; (B) PEO extracted scaffold. Scale bars are 2 μm.

a porous network. The extraction of PEO did not significantly affect the morphology or diameter of the fibers.

3.2. Cell proliferation, metabolic activity and viability on ESFS

Good retention of vascular cells on seeded grafts is a critical issue for clinical transplantation [19,20]. The assessment of the retention of endothelial and smooth muscle cells on ESFS in vitro can provide initial confirmation of the utility of this new system. The growth and metabolic behavior of both HCASMCs and HAECs on the ESFS was characterized by Pico green™ DNA content and alamarBlue™ assays, respectively. To observe cell growth on the ESFS, high cell seeding density was used for the HCASMCs (2.5×10^5 cells/cm^2) and DNA content and metabolic activity was determined at days 1, 5, 10, 15, 21, 25, 32 and 36. A significant increase in DNA content was observed at day 5 compared to day 1, and steady growth was observed after day 5 (Fig. 3A). The metabolic activity profile of HCASMCs was different than the cell proliferation profile (Fig. 3B). An increase in cell activity was observed after day 1 and maximum metabolism was reached over 10 days. Activity ended at 66% of initial level on day 36. The viability of HCASMCs was examined by confocal microscopy after live/dead staining, and high viability over the
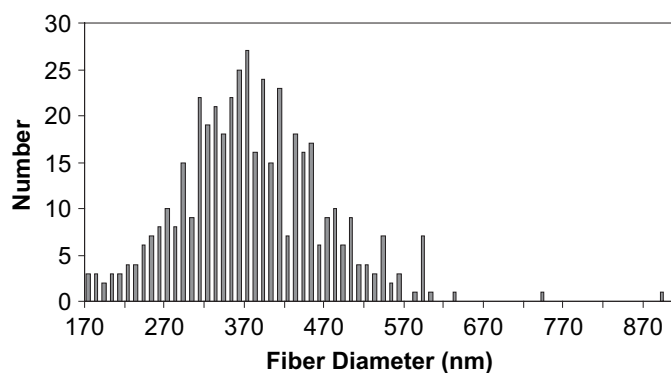

Fig. 2. Histograms of electrospun silk fibroin scaffolds fiber diameters after PEO extracted.

36-day culture was demonstrated, with metabolic activity decreasing toward the end of the culture period (Fig. 4).

For the HAECs, metabolic activity and viability at day 1, 4, 7 and 14 was assessed. Increasing DNA content was observed from day 1 to day 7, with no subsequent significant growth, representing confluence reached around day 7 (Fig. 5A). Similar metabolic activity of HAECs was maintained when the cells were proliferating during the first week (Fig. 5B), while more than a 2-fold increase was observed on day 14, compared to day 7, although the DNA content was fairly constant after day 7. Viability of the HAECs was maintained over the 14-day culture period as exhibited by confocal microscopy (Fig. 6).

3.3. Cell morphology on ESFS

The morphology of cells on the ESFS was characterized by SEM and confocal microscopy. Significant cell morphology changes with time in culture were observed for both cell types. The HCASMCs demonstrated random orientation with a more spread and stellate state after 1 day in culture (Fig. 4A) and started to change to spindle-shape with parallel alignment when the cells were cultured for 5 days (Fig. 4B). On day 10, the trend toward elongation was more significant and the cell surface contact area became larger (Fig. 4C–F). Single cell morphology was difficult to discern due to the cell confluence on the scaffolds, the elongation and spreading of the HCASMCs was still revealed by the difference in the cell morphology by SEM micrographs (Fig. 7). However, alignment became less significant after 32 days in culture (Fig. 4G,H). Many studies have shown cell alignment (including smooth muscle cells) on the electrospun scaffolds with aligned patterns, compared to randomly oriented scaffolds [21–23]. However, in the present study, alignment of HCASMCs was observed on a randomly oriented non-woven fibrous scaffold. This could be a characteristic "hill and valley" distribution of smooth muscle cells, usually self-organized as soon as they become confluent. However, the differences in cell orientation and morphology between the top and bottom layers revealed the importance of cell–matrix interactions for cell alignment.
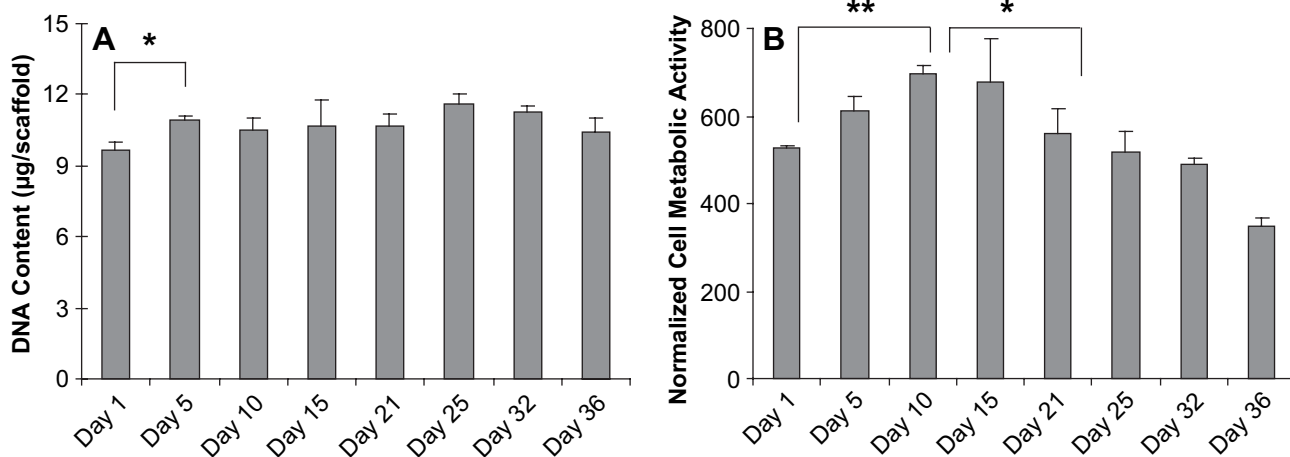
Fig. 3. Human coronary artery smooth muscle cell (HCASMC) proliferation and metabolic activity on electrospun silk fibroin scaffolds. (A) DNA quantification by Pico green™ DNA content assay. A significant increase of DNA content was observed on day 5 (**$p < 0.01$). (B) HCASMC metabolic activity using alamarBlue™ and normalized by DNA content. A significant increase was observed during the first 10 days (**$p < 0.01$) and decreased after day 15 (*$p < 0.05$). Error bars represent mean ± standard deviation with $n = 3$.

The morphology of the HAECs was regular with cobblestone shapes 1 day after cell seeding on the scaffolds (Figs. 6 and 8). Multiple protrusions and the first sign of small aggregates of aligned cells forming short cord-like structures without identifiable lumen were observed at day 4 (Fig. 6B). Over time from day 7 to day 14, a complex interconnecting network of capillary tubes with lumens formed, identified by both SEM and confocal microscopy (Figs. 6C,D and 8C,D). These tubule-like structures has been shown in many in vitro angiogenesis assay studies, which involve the migration and differentiation of endothelial cells in angiogenic pathways, usually achieved by culture of endothelial cells in gel scaffolds of matrix proteins such as collagen [24,25], fibrin [26,27],

fibronectin [28], or Matrigel [29]. The process usually takes several days to weeks depending on the matrix protein and experimental conditions [30,31]. In the present study, we observed similar network formation of capillary-like tubes but on ESFS these network structures were discernible by day 7 (Figs. 6C and 8C).

3.4. Cell phenotypes and ECM production on ESFS

In order to determine if the HCASMCs and HAECs still retain their phenotypes when cultured on the ESFS, characteristic protein markers were studied by immunocytochemistry. Confocal microscopy showed that the HCASMCs on the
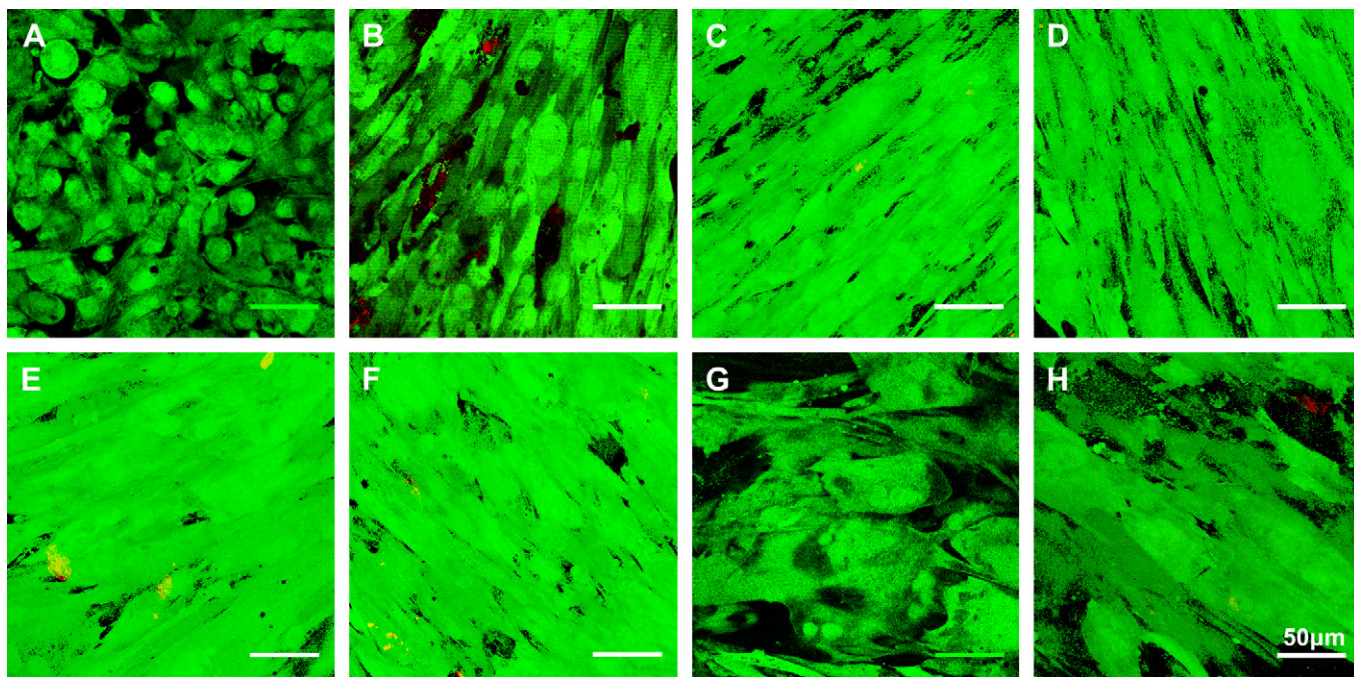

Fig. 4. The viability of HCASMCs on electrospun silk fibroin scaffolds using live/dead assay with confocal microscopy on day 1, 5, 10, 15, 21, 25, 32, 36. High viability was maintained and cell alignment was observed from day 5 (B). Scale bars are 50 μm.
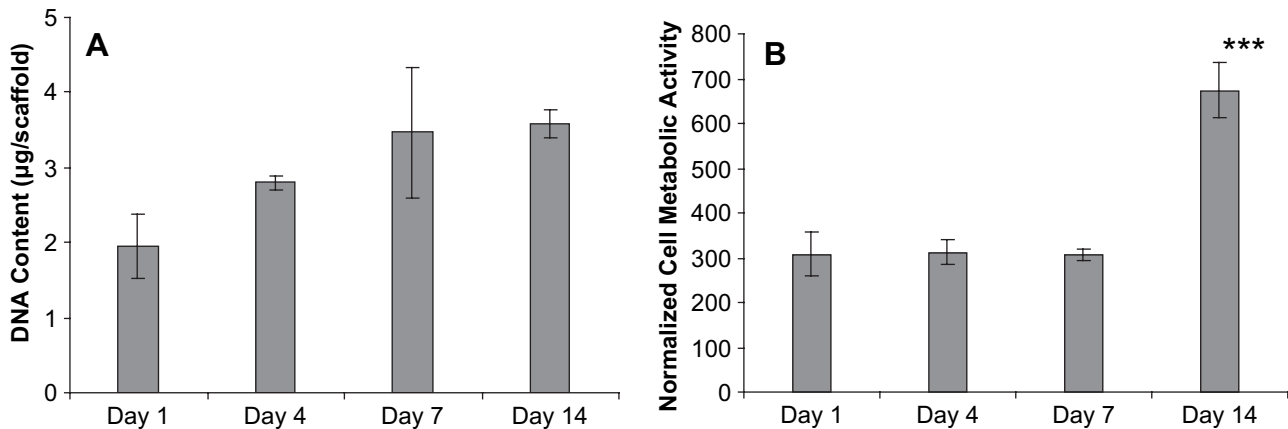
Fig. 5. Human arotic endothelial cell (HAEC) proliferation and metabolic activity on electrospun silk fibroin scaffolds. (A) DNA quantification of HAECs using Pico green™ DNA content assay. No significant increase in DNA content was observed. (B) HAEC metabolic activity using alamarBlue™ and normalized by DNA content. A significant increase was observed on day 14 (***$p < 0.001$). Error bars represent mean ± standard deviation with $n = 3$.

scaffolds stained positive for SM α-actin and SM-MHC2 (a contractile phenotypic marker of SMCs), characteristic proteins for smooth muscle cells (Fig. 9A–H), however, the intensity of the fluorescence diminished after 15 days in culture (data not shown). Generally, smooth muscle cells dedifferentiate from a contractile phenotype to a synthetic phenotype when they are cultured in vitro and lose their phenotype with decreased expression of SM-actin. The ESFS supported smooth muscle cell contractile phenotype. Collagen type I and elastin, important for functional vascular grafts, were assessed by immunocytochemistry. The expression of collagen type I on the silk fibroin scaffolds was aligned, likely reflecting the alignment of the HCASMCs (Fig. 9I–L). This was consistent with what was observed for bladder tissue where the natural alignment of the collagen network reflected the orientation of the smooth muscle cell bundles. The production of elastin was less than the expression of collagen type I (data not shown), however, positively staining for this ECM marker was found.

For HAECs, the expression of the universal EC markers such as CD146, VE-cadherin and PECAM-1 were studied by immunocytochemistry to examine the differentiation status of endothelial cells (Fig. 10). HAECs stained positively for all 3 markers compared to controls, indicating the preservation of EC characteristic phenotype. The interconnecting network of

capillary tubes was also observed from the immunostained micrographs and the cell–cell and cell–matrix interactions were much more distinct on day 14, compared to the first week.

3.5. Cell-characteristics and ECM gene expression

The expression of EC-specific markers at the mRNA level was examined for HAECs cultured on the scaffolds using real-time RT-PCR (Fig. 11). Transcript expression of CD146, vWF and VE-cadherin did not change significantly during the first week in culture, while significant upregulation for all 3 transcripts was observed at day 14, with 1.7, 1.6 and 2.1-fold increases for CD146, vWF and VE-cadherin, respectively, (compared to day 1 levels). The production of collagen type I and elastin for HCASMCs on the scaffolds was also analyzed at transcript levels. Stable levels were found for collagen type I after 21 days and elastin for 15 days in culture, respectively (Fig. 12). Significant downregulation of expression was observed for both ECM-related transcripts following the constant expressions over time.

4. Conclusions

The feasibility of utilizing electrospun silk fibroin scaffolds for vascular tissue engineering was assessed. The electrospun
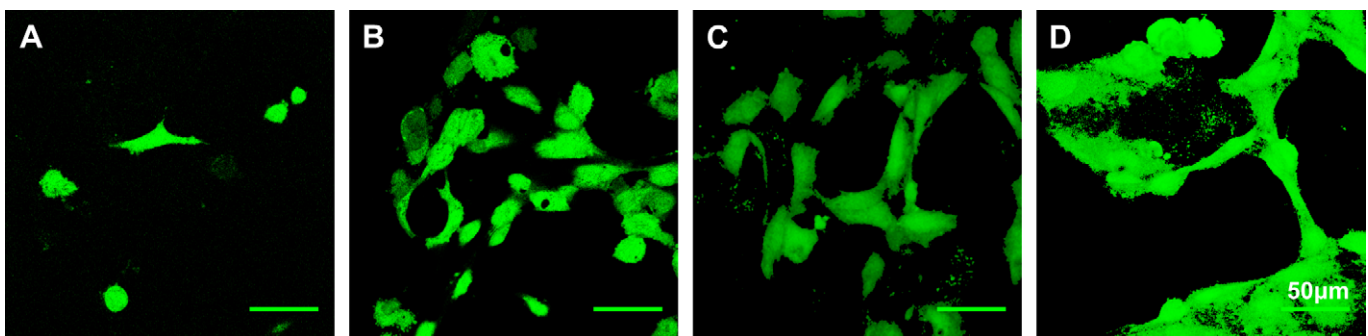

Fig. 6. The viability of HAECs on the electrospun silk fibroin scaffolds using live/dead assay with confocal microscopy on day 1, 4, 7, 14 (A). Viability was maintained and short cord-like structures were observed at day 4 (B), and a complex interconnecting network of capillary tubes with identifiable lumens was demonstrated from day 7 (C,D). Scale bars are 50 μm.
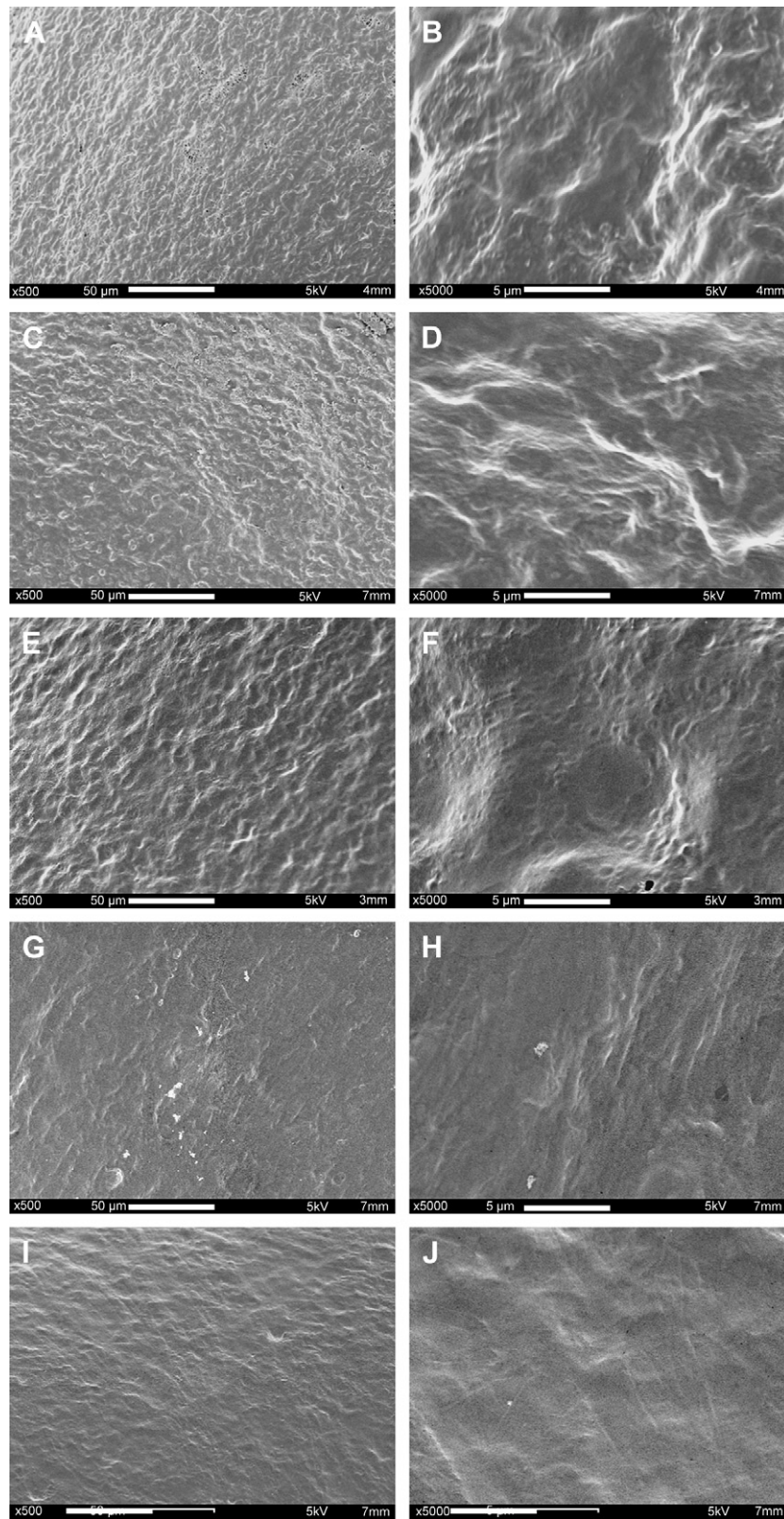
Fig. 7. SEM micrographs of HCASMCs grown on electrospun silk fibroin scaffolds at day 1 (A, B), day 5 (C, D), day 15 (E, F), day 25 (G, H) and day 32 (I, J). Scale bars are: (A, C, E, G, I) 50 μm; (B, D, F, H, J) 5 μm.
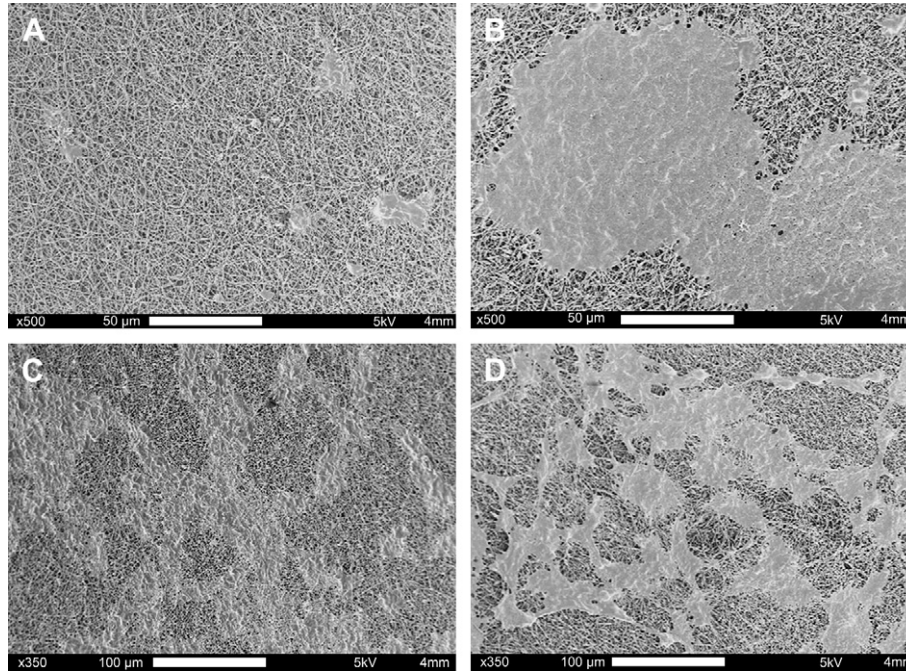
Fig. 8. SEM micrographs of HAECs grown on the electrospun silk fibroin scaffolds at day 1, 4, 7 and 14 (A–D). Scale bars are: (A, B) 50 μm; (C, D) 100 μm.
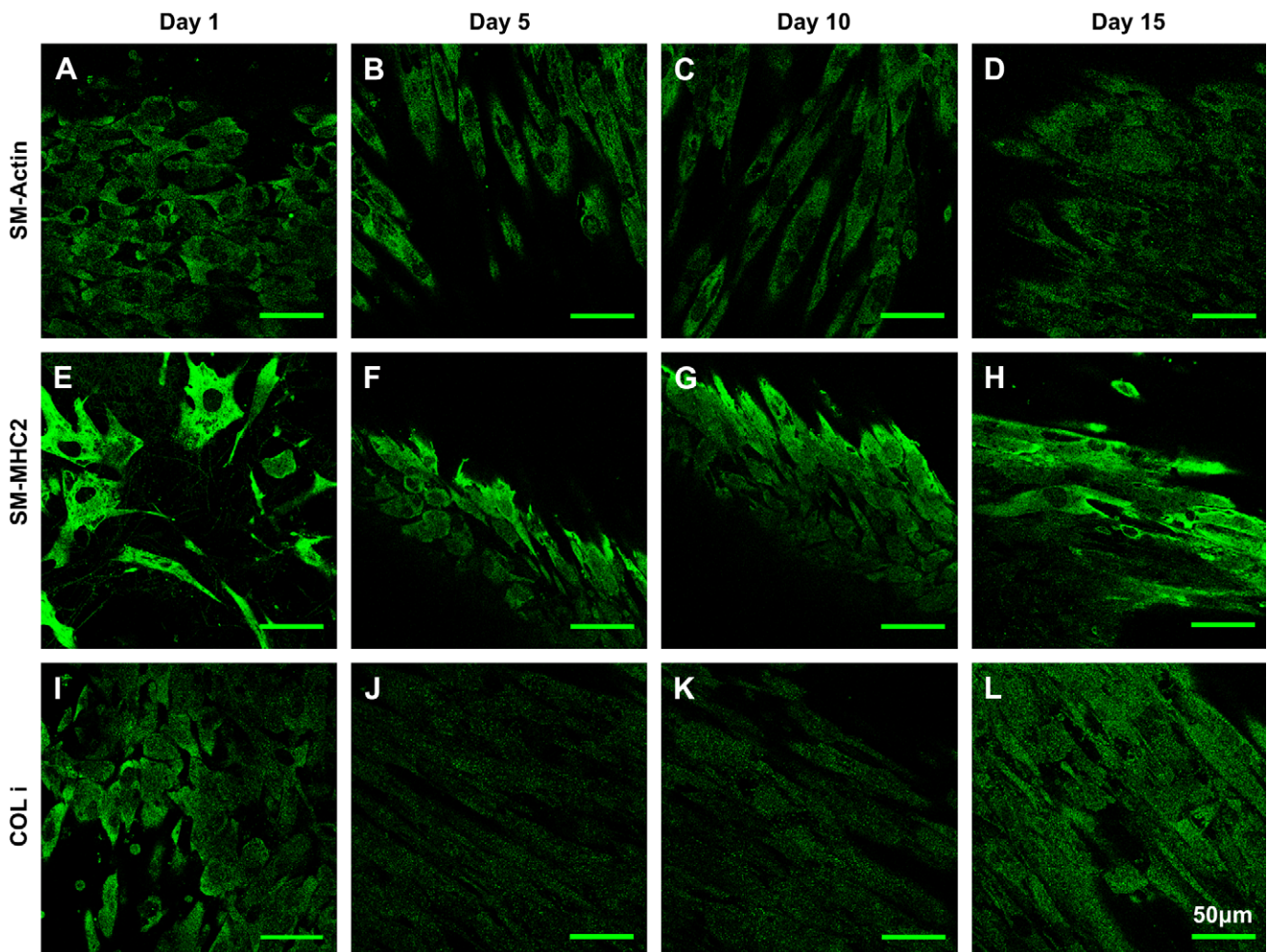

Fig. 9. Immunocytochemistry staining of HCASMCs on electrospun silk fibroin scaffolds at day 1, 5, 10 and 15. Scale bars are 50 μm. Abbreviations: SM-actin: smooth muscle actin; SM-MHC2: smooth muscle myosin heavy chain 2; COL I: collagen type I.
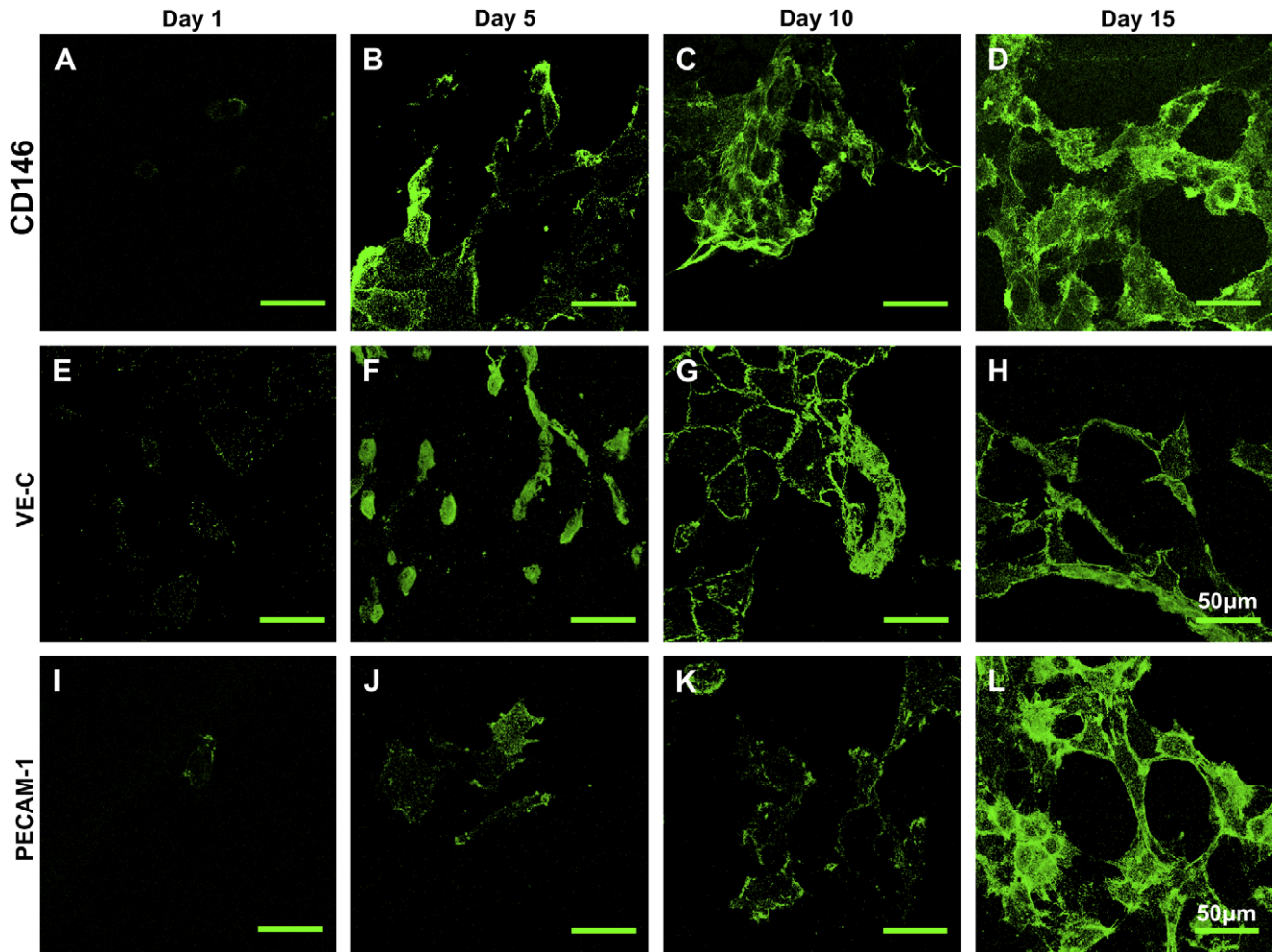
Fig. 10. Immunocytochemistry staining of HAECs on electrospun silk fibroin scaffolds at day 1, 4, 7 and 14. Scale bars are 50 μm. Abbreviations: VE-C: vascular endothelial cadherin.

silk fibroin scaffolds supported the growth and expansion of human aortic endothelial cells and human coronary artery smooth muscle cells based on cell proliferation, morphology and phenotype studies *in vitro*. The results suggest the potential

of these scaffolds for exploration of tissue-engineered vascular grafts, since they support vascular cell viability, maintain cell phenotype and promote cell reorganization. We have previously shown that these electrospun silk systems can be formed into
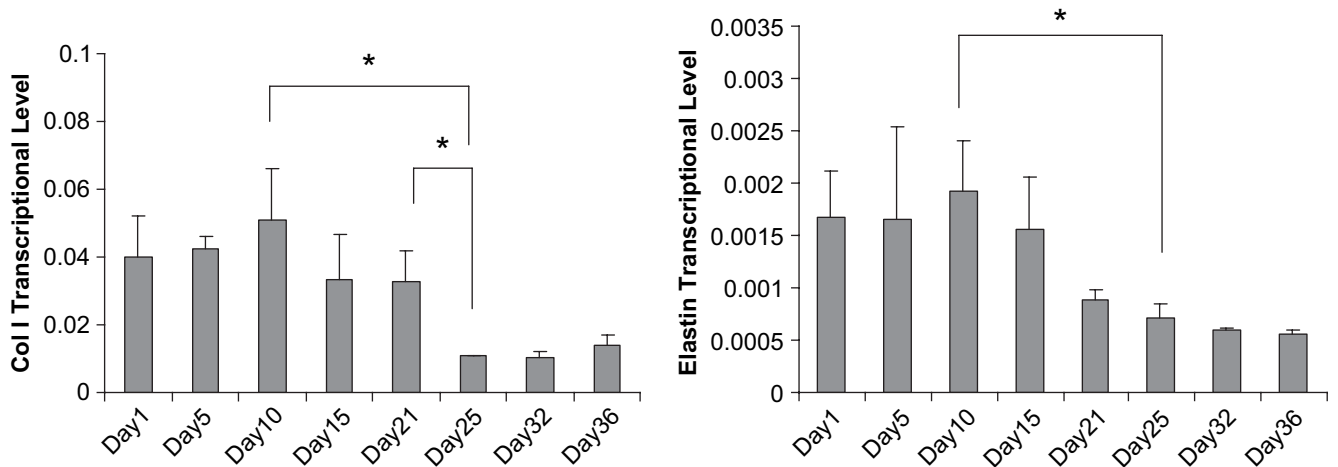

Fig. 11. Transcript levels for HAECs at day 1, 4, 7 and 14 by real-time RT-RCR normalized by GAPDH within the linear range of amplification. Error bars represent mean ± standard deviation with $n = 3$ (*$p < 0.05$, **$p < 0.01$, ***$p < 0.001$).
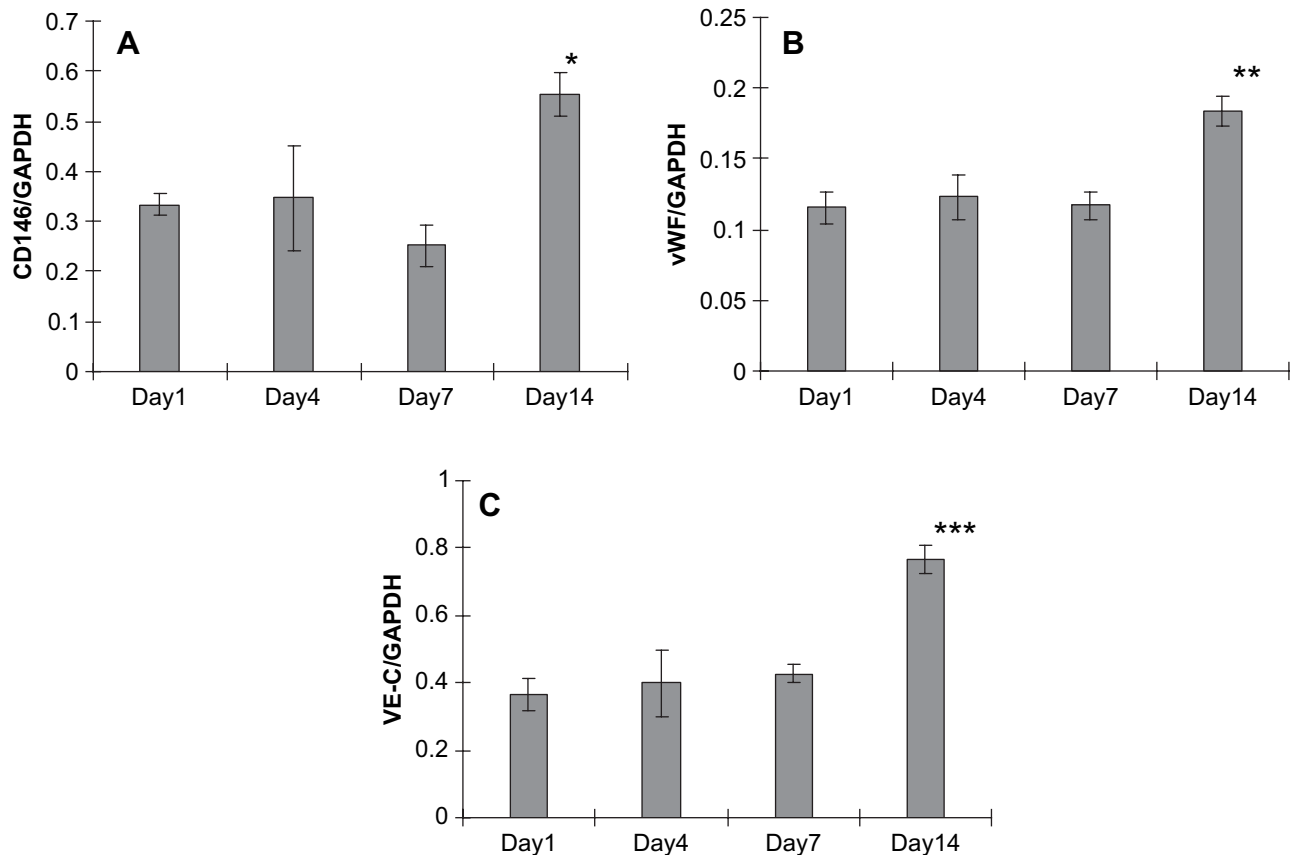
Fig. 12. Transcript levels for HCASMCs at day 1, 5, 10 and 15 by real-time RT-RCR normalized by GAPDH within the linear range of amplification. Error bars represent mean ± standard deviation with $n = 3$ (*$p < 0.05$).

tubular materials with sufficient mechanical integrity to support vascular pressures. Thus future studies are aimed at functional tissue-engineered small-diameter blood vessels by building on the results in the present study.

Conflict of interest

No known conflicts of interest associated with this publication and there has been no significant financial support for this work that could have influenced its outcome.

Acknowledgements

References

[1] Conte MS. The ideal small arterial substitute: a search for the Holy Grail? FASEB J 1998;12:43–5.

[2] Davie EW. Biochemical and molecular aspects of the coagulation cascade. Thromb Haemost 1995;74:1–6.

[3] Nerem RM, Seliktar D. Vascular tissue engineering. Annu Rev Biomed Eng 2001;3:225–43.

[4] Kim BS, Nikolovski J, Bonadio J, Smiley E, Mooney DJ. Engineered smooth muscle tissues: regulating cell phenotype with the scaffold. Exp Cell Res 1999;251:318–28.

[5] Shum-Tim D, Stock U, Hrkach J, Shinoka T, Lien J, Moses MA, et al. Tissue engineering of autologous aorta using a new biodegradable polymer. Ann Thorac Surg 1999;68:2298–305.

[6] Hoerstrup SP, Kadner A, Breymann C, Maurus CF, Guenter CI, Sodian R, et al. Living, autologous pulmonary artery conduits tissue engineered from human umbilical cord cells. Ann Thorac Surg 2002;74:46–52.

[7] Shin'oka T, Imai Y, Ikada Y. Transplantation of a tissue-engineered pulmonary artery. N Engl J Med 2001;344:532–3.

[8] Wake MC, Gupta PK, Mikos AG. Fabrication of pliable biodegradable polymer foams to engineer soft tissues. Cell Transplant 1996;5:465–73.

[9] Isenberg BC, Williams C, Tranquillo RT. Small-diameter artificial arteries engineered in vitro. Circ Res 2006;6(98):25–35.

[10] Seliktar D, Black RA, Vito RP, Nerem RM. Dynamic mechanical conditioning of collagen–gel blood vessel constructs induces remodeling in vitro. Ann Biomed Eng 2000;28:351–62.

[11] Karageorgiou V, Tomkins M, Fajardo R, Meinel L, Snyder B, Wade K, et al. Porous silk fibroin 3-D scaffolds for delivery of bone morphogenic protein-2 in vitro and in vivo. J Biomed Mater Res 2006;78A:324–34.

[12] Wang YZ, Blasioli DJ, Kim HJ, Kim HS, Kaplan DL. Cartilage tissue engineering with silk scaffolds and human articular chondrocytes. Biomaterials 2006;27:4434–42.

[13] Soffer Leah, Wang Xianyan, Zhang Xiaohui, Kluge Jonathan, Dorfmann Luis, Kaplan David L., et al. Silk-based electrospun tubular scaffolds for tissue-engineered vascular grafts. J Biomater Sci Polym Ed, in press.

[14] Kim UJ, Park JH, Kim HJ, Wada M, Kaplan DL. Three-dimensional aqueous-derived biomaterial scaffolds from silk fibroin. Biomaterials 2005;26:2775–85.

[15] Jin H-J, Chen J, Karageorgiou V, Altman GH, Kaplan DL. Human bone marrow stromal cell responses on electrospun silk fibroin mats. Biomaterials 2004;25(6):1039–47.

[16] Huang L, Nagapudi K, Apkarian RP, Chaikof EL. Engineered collagen–PEO nanofibers and fabrics. J Biomater Sci Polym Ed 2001;12:979–93.

[17] Buttafoco L, Kolkman NG, Engbers-Buijtenhuijs P, Poot AA, Dijkstra PJ, Vermes I, et al. Electrospinning of collagen and elastin for tissue engineering applications. Biomaterials 2006;27:724–34.

[18] Kidoaki S, Kwon IK, Matsuda T. Mesoscopic spatial designs of nano- and microfiber meshes for tissue-engineering matrix and scaffold based on newly devised multilayering and mixing electrospinning techniques. Biomaterials 2005;26:37–46.

[19] Bhat VD, Klitzman B, Koger K, Truskey GA, Reichert WM. Improving endothelial cell adhesion to vascular graft surfaces: clinical need and strategies. J Biomater Sci Polym Ed 1998;9:1117–35.

[20] Herring MB. Endothelial cell seeding. J Vasc Surg 1991;13:731–2.

[21] Yang F, Murugan R, Wang S, Ramakrishna S. Electrospinning of nano/micro-scale poly(L-lactic acid) aligned fibers and their potential in neural tissue engineering. Biomaterials 2005;26:2603–10.

[22] Lee CH, Shin HJ, Cho IH, Kang YM, Kim IA, Park KD, et al. Nanofiber alignment and direction of mechanical strain affect the ECM production of human ACL fibroblast. Biomaterials 2005;26:1261–70.

[23] Zong X, Bien H, Chung CY, Yin L, Fang D, Hsiao BS, et al. Electrospun fine-textured scaffolds for heart tissue constructs. Biomaterials 2005;26:5330–8.

[24] Baker SC, Atkin N, Gunning PA, Granville N, Wilson K, Wilson D, et al. Characterisation of electrospun polystyrene scaffolds for three-dimensional in vitro biological studies. Biomaterials 2006;27:3136–46.

[25] Sweeney SM, Guy CA, Fields GB, San Antonio JD. Defining the domains of type I collagen involved in heparin-binding and endothelial tube formation. Proc Natl Acad Sci USA 1998;95:7275–80.

[26] Montanez E, Casaroli-Marano RP, Vilaro S, Pagan R. Comparative study of tube assembly in three-dimensional collagen matrix and on Matrigel coats. Angiogenesis 2002;5:167–72.

[27] Collen A, Koolwijk P, Kroon M, Van H, Victor WM. Influence of fibrin structure on the formation and maintenance of capillary-like tubules by human microvascular endothelial cells. Angiogenesis 1998;2:153–66.

[28] Nakatsu MN, Sainson RCA, Aoto JN, Taylor KL, Aitkenhead M, Perez-del-Pulgar S, et al. Angiogenic sprouting and capillary lumen formation modeled by human umbilical vein endothelial cells (HUVEC) in fibrin gels: the role of fibroblasts and angiopoietin-1. Microvasc Res 2003;66:102–12.

[29] Ingber DE, Folkman J. Mechanochemical switching between growth and differentiation during fibroblast growth factor-stimulated angiogenesis in vitro: role of extracellular matrix. J Cell Biol 1989;109:317–30.

[30] Auerbach R, Auerbach W, Polakowski I. Assays for angiogenesis: a review. Pharmacol Ther 1991;51:1–11.

[31] Gamble JR, Matthias LJ, Meyer G, Kaur P, Russ G, Faull R, et al. Regulation of in vitro capillary tube formation by anti-integrin antibodies. J Cell Biol 1993;121:931–43.